

## An investigation on initial dilution of thermal wastewater discharges into shallow receiving waters with 60° inclination

Ugur Emre Temelli<sup>a</sup>, Naim Sezgin<sup>b</sup>, Fatma Djamaa<sup>b</sup>, Semih Nemlioglu<sup>b,\*</sup>

<sup>a</sup>Istanbul University, Vocational School of Technical Sciences, Property Protection and Security Department, Civil Defense and Fire Fighting Program, 34320, Avcilar, Istanbul, Turkey, Tel. +90 212 473 70 70/18188, Fax. +90 212 473 70 79, email: uetemelli@gmail.com

<sup>b</sup>Department of Environmental Engineering, Faculty of Engineering, Istanbul University, 34320 Avcilar, Istanbul, Turkey, Tel. +90 212 473 70 70/17735, Fax. +90 212 473 71 80, email: nsezgin@istanbul.edu.tr (N. Sezgin), biofat88@yahoo.fr (F. Djamaa), snemli@istanbul.edu.tr (S. Nemlioglu)

Received 16 June 2017; Accepted 28 September 2017

### ABSTRACT

In this study, effects of shallow water depths on initial dilution levels of heated water discharge from thermal effluent outfalls concerning water surface boundary effects using an inclined circular port were investigated. Receiving water environment was selected as stagnant and uniform characteristics. The inclination angle of discharge port was  $\theta = 60^\circ$ . Normalized port depths,  $H/dF$ , which was obtained from water depth ( $H$ ) over port diameter ( $d$ ) multiplied by densimetric Froude number ( $F$ ) of jet defined as  $dF$ , were calculated for experimental set-ups.  $H/dF$  values were 3.871, 1.545, 1.160, 0.774, and 0.388 from deep to shallower depths, respectively. Rhodamine B was used as tracer of experiments. Normalized forms of impingement point horizontal distance values,  $x/dF$ , and vertical distance values,  $y/dF$  were decreased according to decreased water depths,  $H/dF$ . According to obtained results of this study, jet impingements occurred in the upper boundary of the receiving water body and they got closer to the nozzle when  $H/dF$  values decreased. In addition, the decreasing  $H/dF$  values caused a decrease in dilutions of horizontal distances for both complete jet centerlines (especially impact points compared to experimental) and VP estimates of free jet conditions. According to this study, VP dilution estimations were found very close to experimental impingement point dilutions no matter how VP software originally designed for only free jet conditions. This study suggests VP UM3 model can calculate realistic and conservative jet centerline dilutions at the impingement point in very limited depths in the range of normalized water depth ratio  $H/dF$  between 0.388 and 1.545.

**Keywords:** Thermal outfall; Visual plumes; Positively buoyant jet; Initial dilution; Restricted discharge depth; Impact point dilution; Nozzle inclination

### 1. Introduction

Thermal effluents into natural water bodies (rivers, lakes and seas) are discharged from some industries such as power plants by means of outfalls and diffusers. These effluents change ambient water temperature, and cause detrimental effects to aquatic creatures due to the limited temperature tolerance of most of the aquatic species [1–3]. The heated wastewater forms a vast majority of thermal discharges (of course, the other part of thermal discharges

are cold wastewaters) and it is released from the open cycle cooling water systems of power plants and industrial facilities [4,5]. Power plants discharge more heated wastewater than any other industrial facilities because they use a lot of water during the cooling process [6]. After the cooling water is used at thermal power plants, it is discharged as heated wastewater into the receiving water body. When this heated wastewater mixes with the receiving ambient water body, creates a thermal plume. The heated wastewater can increase the receiving ambient temperature which can cause adverse effects to living organisms [7].

\*Corresponding author.

Presented at the 3rd International Conference on Recycling and Reuse, 28-30 September 2016, Istanbul, Turkey

In order to prevent these undesired effects, temperature change effects in the receiving water body must be limited and regulated. To obey these regulation limitations efficiently, initial dilution and mixing by multiport diffusers should be used in heated water marine outfall systems. The mixing of thermal discharge in the receiving ambient water body is influenced by ambient turbulent shear and boundary interaction including flow impingements and dynamic attachments. There are two mixing process, near-field and far-field, for discharging the wastewater into the receiving ambient water. An initial near-field mixing process consists of turbulent jet mixing followed by mixing due to buoyancy effects. Far-field mixing occurs after the effluent field has moved out of the influence of near port jet and momentum effects have stabilized at the trapping depth, or reached the surface. This includes continued dilution due to buoyant spreading and passive diffusion depending on turbulent shear force in the ambient flow. Buoyancy delays the transition to far-field passive diffusion and mixing is relatively small in buoyant spreading. Therefore, a comprehensive understanding of hydrodynamic initial mixing processes including boundary interactions of discharged wastewaters is prerequisite for controlling wastewater discharges into, and minimizing the impact on, the aquatics environment [1,8].

The surface boundary interaction is an important process for heated wastewater dilutions especially in shallow locations. Contrary to this importance, there is limited literature on surface boundary impact and thermal discharges into the receiving water body. Because of economic reasons, discharge depths of heated wastewater can be desirable at shallow locations. At this condition, the discharged heated wastewater will be hitting the jets at the upper boundary of receiving ambient water surface earlier than in deeper conditions. However, the initial dilution performances of heated wastewater jets at the impingement point are not well known, they need to be investigated. Therefore, in this study, effects of the water surface boundary interactions on initial dilution levels of heated wastewater discharge were investigated at different shallow water depths. All the experimental data sets were also compared to dilution results of UM3 model of US EPA surface water discharge model system software, Visual Plumes (VP), for free thermal jet conditioned identical cases of the performed experiments.

## 2. Materials and methods

In this study, a series of heated wastewater jets from inclined single port at an inclination angle,  $\theta = 60^\circ$ , were discharged into stagnant and uniform receiving water body with  $\Delta T_0 = +5^\circ\text{C}$  initial temperature change by an inclined circular port in the experimental tank which was located in studied laboratory. Port depths were selected as  $H = 5, 10, 15, 20, 50$  cm. Rhodamine B was used as tracer to observe the heated wastewater behaviors. The sketch of the discharging port is given in Fig. 1. Analysis of positively buoyant flow regime and some discharge characteristics such as kinematic fluxes of volume, momentum, and buoyancy have been reported in previous studies by Sezgin [3] and Toyoshima and Okawa [9]. All normalized jet parameters are summarized in Table 1. Also, densimetric Froude number

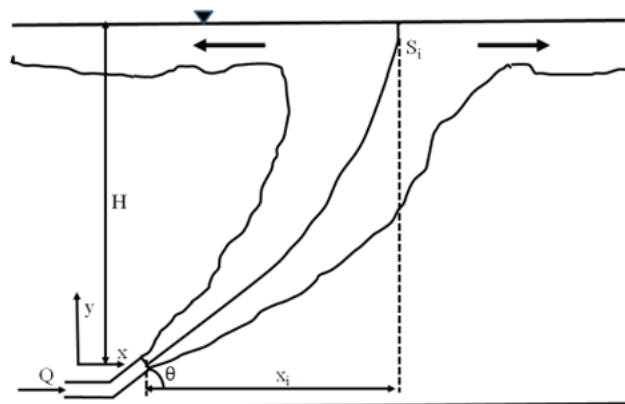


Fig. 1. Sketch of  $60^\circ$  inclined heated jet discharge.

Table 1  
Experimental parameters in normalized form

Definitions	Parameters
Depth of nozzle center	$H/dF$
Local jet centerline horizontal distance from nozzle center	$x/dF$
Local jet centerline vertical distance from nozzle center	$y/dF$
Horizontal distance of impact point from nozzle center	$x_i/dF$
Local dilution in jet centerline	$S_m/F$
Impact point dilution	$S_i/F$

(F) to which dilution and jet geometrical features depend on, are defined using the following Eq. (1) and Eq. (2):

$$F = \frac{u}{\sqrt{g \cdot d \cdot \left(\frac{\Delta\rho}{\rho_0}\right)}} \quad (1)$$

$$\Delta\rho = \rho_0 - \rho_a \quad (2)$$

where  $u$ : jet exit velocity,  $d$ : discharge nozzle diameter,  $g$ : gravitational acceleration,  $\rho_0$ : effluent density,  $\rho_a$ : ambient density and  $\Delta\rho$ : difference of water densities. By using Eqs. (3)–(5) local jet centerline dilutions  $S_m$  were obtained:

$$S_m = \Delta T_0 / \Delta T_m \quad (3)$$

$$\Delta T_0 = T_0 - T_a \quad (4)$$

$$\Delta T_m = T_m - T_a \quad (5)$$

where  $\Delta T_0$  is the temperature difference at discharge nozzle,  $T_a$  is temperature of ambient water, and  $T_0$  is discharged water temperature,  $\Delta T_m$  is the maximum temperature difference in any of local cross section of the jet centerline. The initial temperature change values were all set at  $\Delta T_0 = +5^\circ\text{C}$  in this study. The length scale parameters, such as  $H, x, y$ ,

and  $x_i$  were divided by  $dF$  (port diameter ( $d$ ) multiplied by densimetric Froude number) for normalization. Other normalized parameters without length scale were only divided by densimetric Froude number,  $F$  as shown in Table 1.

The heated water mixed with Rhodamine B tracer was discharged by pumping it into the experiment tank filled with fresh water. Rhodamine B concentration was 0.1 g/L. Firstly, the heated water jet was allowed to reach water surface freely and the flow was photographed when a stable regime was obtained. Then, a series of temperature sensors connected to a mobile mechanism were immersed into the jet to determine temperature distribution in the jet cross-section and the jet centerline coordinates via a scanning method. In these measurements, seven PT100 temperature sensors with 4 mm diameter and 3 cm length were placed within 10 cm distance to each other with a Lufft Opus 200 device. Heating process was prepared by PolyScience digital water bath, where initial density measurements were made by an Anton Paar DMA 4500 device. The dimensions of the experiment tank were 76.5 cm  $\times$  196 cm  $\times$  119.5 cm (width  $\times$  length  $\times$  height). The top surface of the tank was open while the other surfaces were made of transparent Plexiglas. Discharge port was placed on one of the tank wall at 60°. Discharge flow rate was set by McMillan S-112 digital flow-meter and flow was maintained by Cole-Parmer Master flex pump. Jet centerline coordinates and dilution values were obtained by immersed temperature probes into the heated jet bodies. The summary of the experimental set-up of the conducted 15 experiments is given in Table 2 [10].

Experimentally obtained jet centerline dilutions and their impact point distances were compared with US EPA surface water dilution software Visual Plumes (VP), UM3 model jet centerline. Characteristic discharge parameters of all experiments were entered in VP. All VP obtained results were represented as free jet conditions as reported by Frick et al. [11]. Water depth limited experimental heated jet impingement point normalized vertical position is defined

as  $y_i/dF$ .  $y_i/dF$  values were adopted as  $H/dF$  for VP trajectory estimations, because of the fact that lack of impingement point solutions in VP as reported in its manual user guide [11].

### 3. Results and discussion

In this study discharges of heated water from inclined nozzle ( $\theta = 60^\circ$ ) were evaluated in two main stages; 1. Jet geometry, 2. Dilutions.

#### 3.1. Jet geometry

As shown in Fig. 2, all conducted heated discharges for five different port depths were positively formed in the buoyant jets, as expected. According to Fig. 2, jet impingements occurred in the upper boundary of the water body and they got closer to the nozzle when  $H/dF$  values decreased. After impingement, jets formed density currents on the water surface, and they freely moved without any interaction at the bottom of the tank even in the shallowest conditions.

Local maximum temperature differences and their locations through the experimental tank were determined by three dimensionally scanned cross-sectional temperature measurements in the heated water jets. It was seen that the local maximum temperature difference points were located in middle of the heated water jets. These jet trajectories were defined as jet centerline. The normalized jet centerlines for different water depths and VP created free jet centerline as shown in Fig. 3. The direction changing positions of heated water jet trajectories at the water surface were found as the impingement points and the inside of these points were marked as white color, Fig. 3. Impingement point horizontal distance values,  $x_i/dF$  and vertical distance values,  $y_i/dF$  decreased with decreasing water depths,  $H/dF$  as shown

Table 2  
Experimental set-up summary (Flow regimes as L: Laminar, T: Turbulent) [10]

Experiment No	$T_0$ (°C)	$T_a$ (°C)	$d$ (cm)	H (cm)	H/dF	F	$\rho_a$ (kg/m <sup>3</sup> )	$\rho_0$ (kg/m <sup>3</sup> )	$q$ (mL/min)	$u_0$ (m/s)	Re	Flow Regime
FD-60-01-A	28.4	23.4	0.5	50	3.869	25.84	997.757	996.493	240	0.2037	1269	L
FD-60-01-B	28.4	23.4	0.5	50	3.869	25.84	997.757	996.493	240	0.2037	1269	L
FD-60-01-C	28.5	23.5	0.5	50	3.876	25.79	997.733	996.464	240	0.2037	1269	L
FD-60-02-A	28.3	23.3	0.5	20	1.545	25.89	997.781	996.522	240	0.2037	1269	L
FD-60-02-B	28.3	23.3	0.5	20	1.545	25.89	997.781	996.522	240	0.2037	1269	L
FD-60-02-C	28.3	23.3	0.5	20	1.545	25.89	997.781	996.522	240	0.2037	1269	L
FD-60-03-A	28.3	23.3	0.5	15	1.158	25.89	997.781	996.522	240	0.2037	1269	L
FD-60-03-B	28.5	23.5	0.5	15	1.160	25.79	997.733	996.464	240	0.2037	1269	L
FD-60-03-C	28.4	23.4	0.5	15	1.163	25.84	997.757	996.493	240	0.2037	1269	L
FD-60-04-A	28.4	23.4	0.5	10	0.773	25.84	997.757	996.493	240	0.2037	1269	L
FD-60-04-B	28.6	23.6	0.5	10	0.775	25.75	997.708	996.435	240	0.2037	1269	L
FD-60-04-C	28.5	23.5	0.5	10	0.776	25.79	997.733	996.464	240	0.2037	1269	L
FD-60-05-A	28.4	23.4	0.5	5	0.387	25.84	997.757	996.493	240	0.2037	1269	L
FD-60-05-B	28.6	23.6	0.5	5	0.388	25.75	997.708	996.435	240	0.2037	1269	L
FD-60-05-C	28.6	23.6	0.5	5	0.388	25.75	997.708	996.435	240	0.2037	1269	L

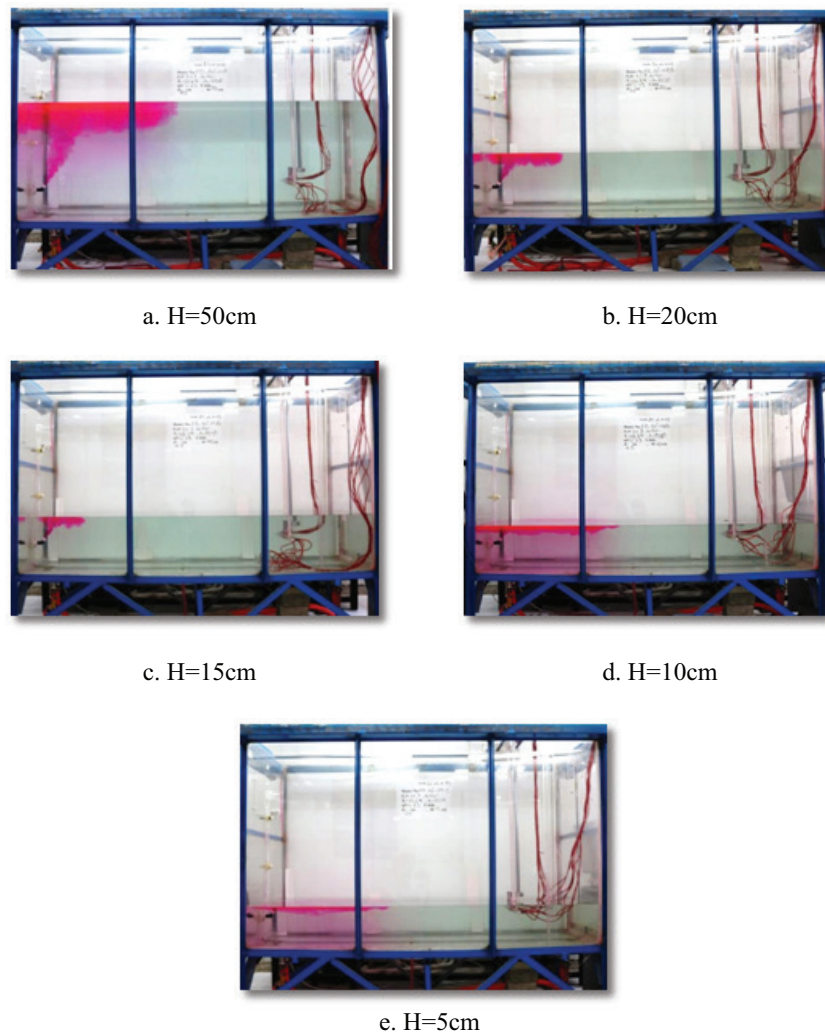


Fig. 2. Heated water discharged at 60° at different water depths.

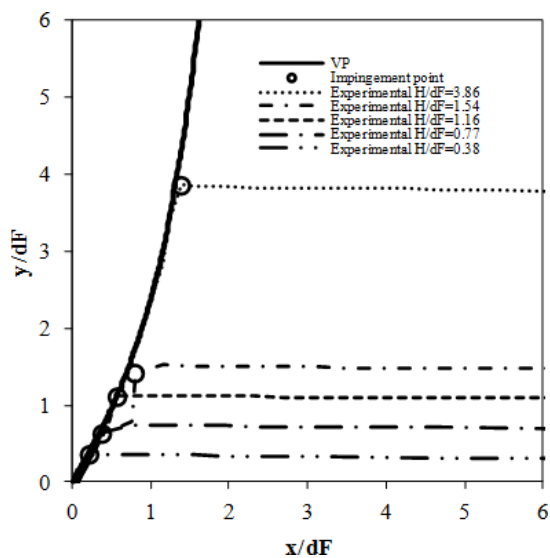


Fig. 3. Average heated water jet trajectories (white markers are impingement points).

in Fig. 3. In addition, all experimental  $x_i/dF$  values did not match exactly VP estimated free jet trajectory. This can be attributed to the heated water jet interaction with the water surface, where the experimental  $x_i/dF$  values are slightly higher than VP estimated free jet  $x/dF$  values at the same vertical positions. Similar relations were also observed for water surface obstructed heated jet  $x_i/dF$  and  $x/dF$  values of free experimental jet at same heights. The comparison between  $H/dF$  and  $y_i/dF$  are given in Table 3. From Table 3,  $y_i/dF$  were found to be lower than  $H/dF$  values because of limited water depth effects on buoyant jets.

### 3.2. Dilution

The heated jet centerline dilution comparisons are given in Fig. 4 for different water depths. VP estimated free jet centerline dilutions of horizontal distances are also presented in Fig. 4. It was shown that, decreasing  $H/dF$  values caused a decrease of dilutions in horizontal distances for both complete jet centerlines (especially impact points compared to the experimental) and VP estimates free jet



Table 3  
Experimental port depth and impinge point parameters relations

Experiment No	H/dF	$x_i/dF$	$y_i/dF$	$S_i/F$
FD-60-01-A	3.869	1.39	3.862	0.64
FD-60-01-B	3.869	1.32	3.846	0.69
FD-60-01-C	3.876	1.28	3.851	0.59
FD-60-02-A	1.545	0.80	1.529	0.42
FD-60-02-B	1.545	0.79	1.536	0.43
FD-60-02-C	1.545	0.83	1.185	0.39
FD-60-03-A	1.158	0.58	1.143	0.35
FD-60-03-B	1.160	0.62	1.046	0.34
FD-60-03-C	1.163	0.54	1.142	0.36
FD-60-04-A	0.773	0.36	0.750	0.22
FD-60-04-B	0.775	0.40	0.587	0.23
FD-60-04-C	0.776	0.42	0.557	0.24
FD-60-05-A	0.387	0.22	0.371	0.14
FD-60-05-B	0.388	0.24	0.344	0.14
FD-60-05-C	0.388	0.21	0.371	0.14

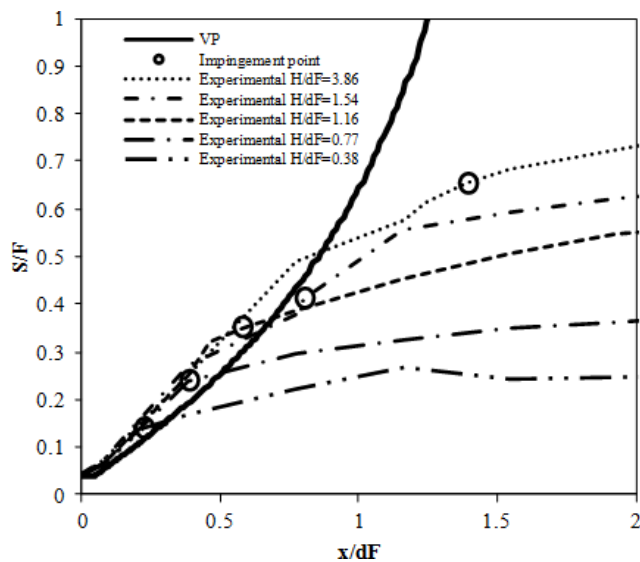


Fig. 4. Comparison of normalized initial dilutions of heated water jet centerlines for horizontal distances at different discharge depths.

Table 4  
Mean values of impingement point parameters comparison with free jet conditions

Experimental				VP (Free jet)			
H/dF	$x_i/dF$	$y_i/dF$	$S_i/F$	S/F Free jet	$\Delta S_i/F$ (%)	$x_i/dF$	$S_i/F$
3.871	1.39	3.853	0.65	–	–	1.32	1.13
1.545	0.81	1.417	0.41	0.50	–18.00	0.74	0.40
1.160	0.58	1.111	0.35	0.37	–5.40	0.59	0.30
0.774	0.39	0.631	0.23	0.24	–4.16	0.42	0.21
0.388	0.22	0.362	0.14	0.16	–12.50	0.22	0.11

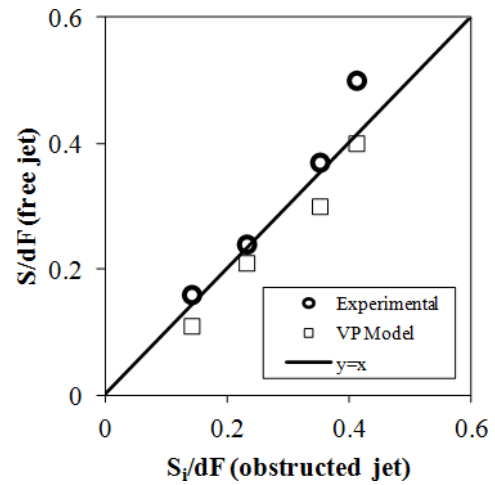


Fig. 5. Comparison of impact point dilutions for obstructed and free jet conditions.

conditions. Impact point dilutions,  $S_i/F$ , were measured as lower values comparing free jet conditioned experimental results. However, VP dilution estimations were kept lower than free jet and even depth limited experimental results in the range 0.388–1.160 of H/dF, Table 4. For experimental results, the rate of impingement point dilution difference between obstructed and free jet,  $\Delta S_i/F$ , were calculated in the range of –4.16% to –18.00% as shown in Table 4.

Comparison of impact point dilutions for obstructed and free jet conditions along  $y = x$  line for both experimental and VP UM3 model estimations is shown in Fig. 5. Because of the fact that H/dF = 3.871 was not free jet at its impingement point, Fig. 5 was only obtained for H/dF values from 0.388–1.545 range. Fig. 5 shows that low S/F values of VP dilution estimations are pretty conservative in shallow water conditions.

#### 4. Conclusion

Heated wastewater outfalls with inclined nozzles can be widely applied to prevent bottom interactions even in positively buoyant jet condition. Because of the economic reasons, heated wastewater discharges can be done in shallow water conditions. However, there are many concerns about water surface impingement related to initial dilution decrease in shallow water conditions. In order to account

for these extreme conditions of very high value of port inclinations were investigated. In this study, heated water discharges were performed at different depth of receiving ambient water body with  $\Delta T_0 = +5^\circ\text{C}$  and the port inclination was selected as  $\theta = 60^\circ$ , which is a very steep angle for this type of arrangement. Water depth decrease effects on initial dilution at  $60^\circ$  inclined heated water discharges were also investigated in this study. Because of water surface boundary effects on heated water jet trajectories, their impingement point related to geometrical parameters were experimentally defined, as well. In order to arrange a useful solution for thermal outfall designers, experimental dilution results were compared to US EPA Visual Plumes UM3 model results for more realistic dilution estimations.

According to this study, there were initial dilution differences between free jet and surface boundary limited jet conditions at impingement points. Obstructed heated water jet initial dilutions were all taken at lower values in the range of  $-4.16\%$  to  $-18.00\%$  compared to free jet conditions. On the other hand, this study also clearly shown that centerline dilution values of US EPA Visual Plumes UM3 model are very close to obstructed initial dilution values in the range of normalized water depth ratio,  $H/dF$  between 0.388 and 1.545. This results shows that Visual Plumes UM3 model impingement point dilution estimations are very conservative and very reliable in shallow water conditions for heated water jets.

#### Acknowledgement

This study, Ministry of Higher Education and Scientific Research of Algeria, management of co-operation and inter-university exchanges under the direction of training and development was supported by abroad scholarship program No. 054 /bis./PG./ TURKEY studies. This work was supported by Scientific Research Project Coordination Unit of Istanbul University. Project number: BEK-2016-20942.

#### References

- [1] S.T. Han, P. Joongcheol, S. Fotis, K. Tarang, Three-dimensional numerical modeling of initial mixing of thermal discharges at real-life configurations, *J. Hydraul. Eng.*, 134(9) (2008) 1210–1224.
- [2] F. Verones, M. Mohdhanafiah, S. Pfister, M.J. Huijbregts, G. Pelletier, A. Dannettekoehler, Characterization factors for thermal pollution in freshwater aquatic environments, *Environ. Sci. Technol.*, 44 (2010) 9364–9369.
- [3] N. Sezgin, Investigation of horizontal cold water discharge initial dilutions at various temperature differences using duck-bill valve, *Desal. Water Treat.*, 57 (2016) 2437–2445.
- [4] P. De Vries, J.E. Tamis, A.J. Murk, M.G.D. Smit, Development and application of a species sensitivity distribution for temperature-induced mortality in the aquatic environment, *Environ. Toxicol. Chem.*, 27(12) (2008) 2591–2598.
- [5] D. Caissie, The thermal regime of rivers: a review, *Freshwater Biol.*, 51(8) (2006) 1389–1406.
- [6] M.A. Maupin, J.F. Kenny, S.S. Hutson, J.K. Lovelace, N.L. Barber, K.S. Linsey, Estimated Use of Water in the United States in 2010; Circular 1405, U.S. Geological Survey: Reston, USA, 2014.
- [7] A. Durán-Colmenares, H. Barrios-Piña, H. Ramírez-León, Numerical modeling of water thermal plumes emitted by thermal power plants, *Water*, 8 (2016) 482–496.
- [8] G.H. Jirka, R.L. Doneker, S.W. Hinton, User's manual for COR-MIX: A hydrodynamic mixing zone model and decision support system for pollutant discharges into surface waters, EPA#: 823/B-97-006, Washington, DC, USA, 1996.
- [9] M. Toyoshima, S. Okawa, An effect of a horizontal buoyant jet on the temperature distribution inside a hot water storage tank, *J. Heat Fluid Flow*, 44 (2013) 403–413.
- [10] F. Djamaa, An investigation on initial dilution of thermal marine outfalls discharging into shallow receiving waters, PhD Dissertation, Institute of Science, Istanbul University, Istanbul, Turkey, 2016 (in Turkish).
- [11] W.E. Frick, Visual Plumes mixing zone modelling software, *Environ. Model. Software*, 19 (2004) 645–654. Available from: <http://www.epa.gov/ceampubl/swater/vplume/>.